

# Chapter 24

## Inelastic Shear Response of RC Walls: A Challenge in Performance Based Design and Assessment

Matej Fischinger, Klemen Rejec, and Tatjana Isaković

**Abstract** The large inelastic shear modification factors proposed in Eurocode for ductile RC walls have been verified and modified. Due to this large amplification, which has, in the past, been ignored, and still is, by many designers, RC walls with insufficient shear resistance have been designed and built. In order to study the seismic vulnerability of such walls, a model was proposed, which takes into account both inelastic shear behaviour and inelastic shear-flexural interaction. It is based on the multiple-vertical-line-element macro model. An additional shear spring, which accounts for aggregate interlock, dowel action and horizontal reinforcement resistance, is incorporated into each of the vertical springs. The model successfully simulated the response of a five-storey coupled wall that was tested on the shaking table under bi-axial excitation. The shear resisting mechanisms within the cracks were adequately modelled up until the tension shear failure of both piers.

**Keywords** RC walls • Coupled wall • Inelastic shear • Inelastic shear/flexural interaction • Shear magnification factors • Eurocode • Multiple-vertical-line-element model

### 24.1 Introduction

For decades, existing numerical models have served the engineering community well. However, the vision of earthquake resilient structures and society itself call for more elaborate and complex tools, which should be able to represent more realistically all possible near-collapse mechanisms. One of the many problems to be solved involves the need for better models and methods for the estimation of the

---

M. Fischinger (✉) • K. Rejec • T. Isaković  
Faculty of Civil and Geodetic Engineering, University of Ljubljana,  
Jamova 2, SI 1000 Ljubljana, Slovenia  
e-mail: [matej.fischinger@fgg.uni-lj.si](mailto:matej.fischinger@fgg.uni-lj.si); [klemen.rejec@fgg.uni-lj.si](mailto:klemen.rejec@fgg.uni-lj.si); [tisak@ikpir.fgg.uni-lj.si](mailto:tisak@ikpir.fgg.uni-lj.si)

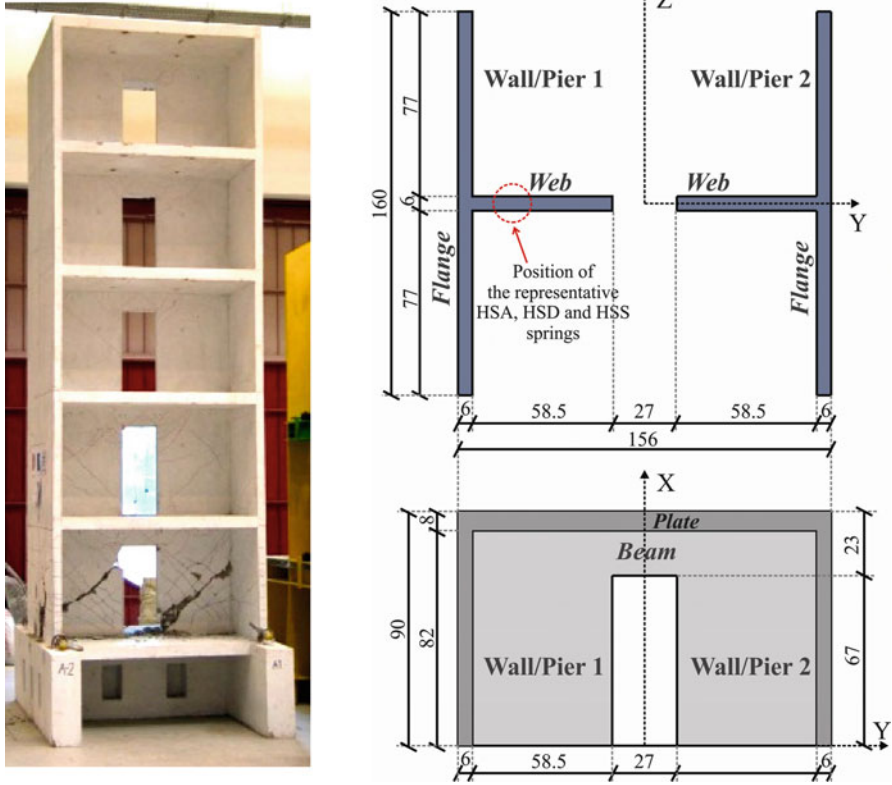


**Fig. 24.1** The wall designed according to Slovenian practice and tested on the shaking table at LNEC in Lisbon (Fischinger et al. 2006)

inelastic shear demand and capacity of reinforced concrete (RC) structural elements. This problem is particularly complex in the case of RC structural walls. The related analyses and observations which are presented in the paper are illustrated by the results of a large-scale shaking table experiment that was performed on a low-rise RC coupled wall (Fig. 24.1). This wall was designed according to the past Slovenian engineering practice (which is similar to that used in Chile).

The wall was modelled and designed to represent part of a typical multi-storey building with structural walls (Fig. 24.2).

Such buildings have been extensively built all over the world, for example in Europe and Chile. This building system is characterized by thin walls and a large wall-to-floor ratio (the structural walls also serve as partition walls). Although, during the recent 2010 Chile earthquake (Boroschek and Bonelli 2014), many compression and shear-compression failures of such walls were observed, the authors believe that this was predominantly due to the misuse of the system beyond its acceptable engineering limits (in particular due to the increasing of the height of the building while keeping the small thickness of the walls unchanged, and the

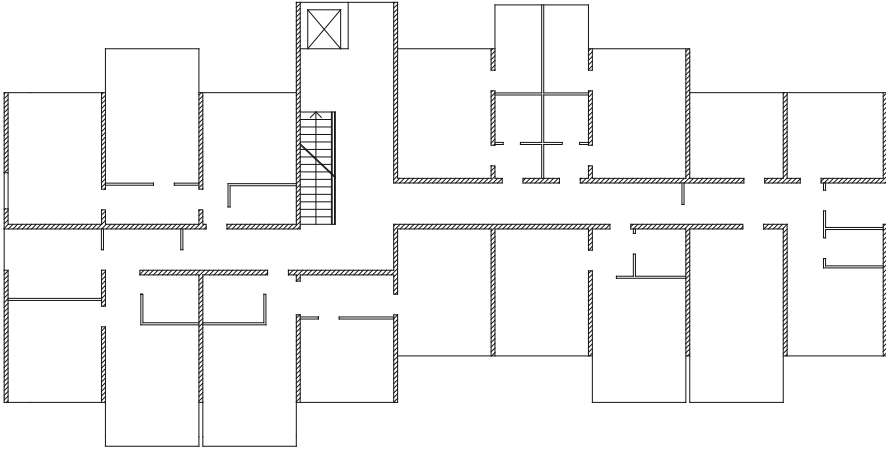


**Fig. 24.2** Typical multi-storey apartment building whose load-bearing structure consists of structural walls



**Fig. 24.3** A pier in a coupled wall damaged during the 1979 Montenegro earthquake

edges lightly confined). If such a system is used for buildings that are not much higher than ten stories, and/or built in moderate seismic regions, the behaviour of the walls should be good, as was observed during several earthquakes in the past (including that which took place in Chile, in 1985) (see Wallace and Moehle 1993). The predominant type of rather rare failures has, in the past, been shear-tension failure (Wood 1991), as is demonstrated in Fig. 24.3, a photograph which was taken after the 1979 Montenegro earthquake. Please note that the common construction practice during the 1970s was to use very weak horizontal reinforcement.

## 24.2 Inelastic Shear Strength Demand in the Design of Cantilever (Wall) Structures

The problem of insufficient shear resistance is not limited just to walls in older buildings. Although a large shear magnification during inelastic response was, long ago, pointed out by Blakeley et al. (1975), even today many designers are not fully aware of this phenomenon and only a few codes, like those used in New Zealand or Eurocode 8 (CEN 2004), consider this magnification explicitly. Eurocode 8 requires that the shear forces obtained by an equivalent elastic analysis  $V_{Ed}'$  are multiplied (over the entire height of the wall) by a shear magnification factor  $\varepsilon$ , in order to obtain the design shear forces  $V_{Ed}$ :

$$V_{Ed} = \varepsilon \cdot V_{Ed}' \quad (24.1)$$

In the case of ductility class high (DCH) walls, the shear magnification factor is determined from the expression (24.2), which was originally proposed by Keintzel (1990):

$$\varepsilon = q \cdot \sqrt{\left(\frac{\gamma_{Rd}}{q} \cdot \frac{M_{Rd}}{M_{Ed}}\right)^2 + 0.1 \cdot \left(\frac{S_e(T_C)}{S_e(T_1)}\right)^2} \begin{cases} \leq q \\ \geq 1.5 \end{cases} \quad (24.2)$$

where:

$q$  is the behaviour (seismic force reduction) factor used in the design;

$M_{Ed}$  is the design bending moment at the base of the wall;

$M_{Rd}$  is the design flexural resistance at the base of the wall;

$\gamma_{Rd}$  is a factor which is used to increase the design value of resistance, accounting for various sources of overstrength;

$T_1$  is the fundamental period of vibration of the building in the direction of action of the shear forces;

$T_C$  is the upper limit period of the constant spectral acceleration region of the spectrum;

$S_e(T)$  is the ordinate of the elastic response spectrum.

In the derivation of this formula, Keintzel assumed that modal combination can also be applied in the inelastic range, and that only the contribution of the first two modes is important:

$$V_{Ed} = \sqrt{(V_{Ed,1})^2 + (V_{Ed,2})^2} \quad (24.3)$$

Keintzel further assumed that energy dissipation could be associated only with the first mode response (within the hinge location at the base, the flexural moment

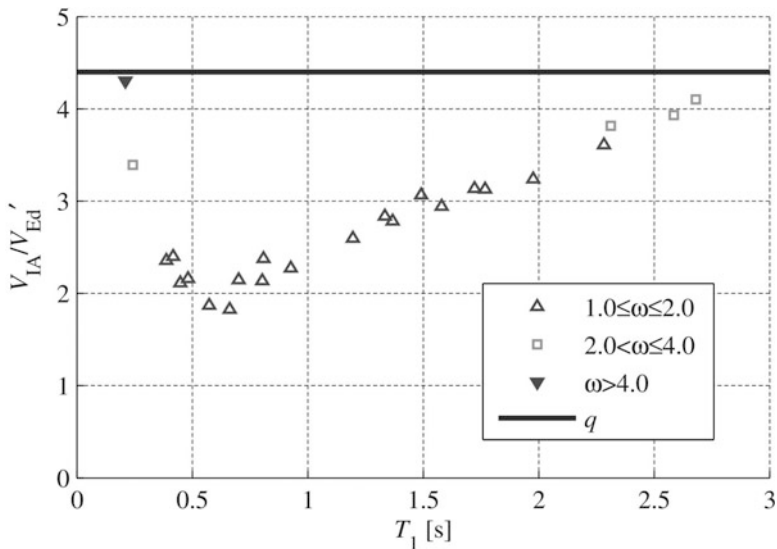


Fig. 24.4 Ratio of the inelastic shear  $V_{IA}'$  and the design shear  $V_{Ed}'$  ( $\omega$  is the flexural overstrength)

due to higher modes is practically negligible). For this reason only the contribution of the first mode should be reduced by the factor  $q$ , whereas the contribution of the second mode should be elastic/unreduced ( $q \cdot V_{Ed,2}'$ ):

$$V_{Ed} = \sqrt{\left(V'_{Ed,1}\right)^2 + \left(q \cdot V'_{Ed,2}\right)^2} \tag{24.4}$$

Considering only the contribution of the first mode to the flexural overstrength (see the previous paragraph), and the ratio of the base shear contributed by the second and the first mode of  $\sqrt{0.1 \cdot S_e(T_2) / S_e(T_1)}$  (in the elastic range), the expression (24.2) was derived.

It should be stressed and clearly understood from the presented derivation that the shear magnification factor  $\epsilon$ , which was proposed by Keintzel (and included in Eurocode 8), should be applied considering only the base shear due the first mode. However, following the ambiguous notation in Eurocode 8, it is most likely that many designers erroneously apply  $\epsilon$  to the total base shear (usually given by commercial computer codes used in design offices).

Recently, a systematic parametric study of the inelastic response of cantilever walls was performed (Rejec et al. 2012) with the aim of studying the adequacy of this shear magnification factor, which had been opposed by many designers as over-conservative. However, the very large increase in shear forces (up to the value of the seismic force reduction factor  $q$ ) was reconfirmed by this study (Fig. 24.4).

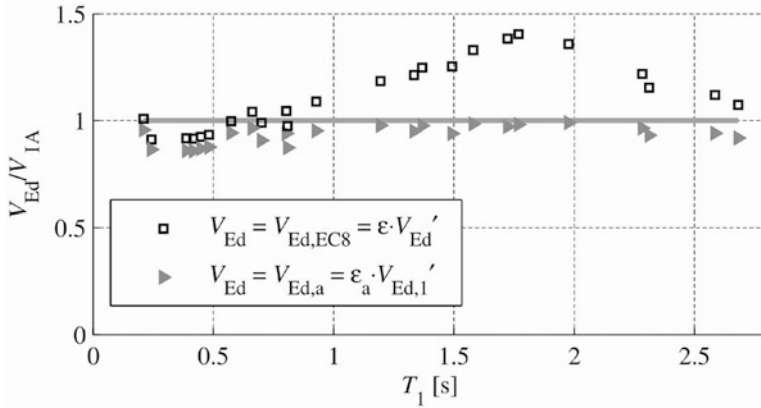


**Fig. 24.5** Design shear forces  $V_{Ed}$  compared to the inelastic shear forces  $V_{IA}$ . The points marked by squares represent the results obtained by the formula given in Eurocode 8, whereas the points marked by triangles represent the results obtained by the proposed formula (24.6)

In (Rejec 2011) it was also demonstrated that:

- (a) In general Keintzel’s formula (used in Eurocode 8) works fine if it is applied correctly (the shear magnification factor is applied to the base shear contributed by the first mode  $V_{Ed,1}$  only).
- (b) However, the upper bound of the shear force should be related to the total base shear ( $V_{Ed,max} = q \cdot V'_{Ed}$ ) and not only to that defined by the first mode contribution ( $V_{Ed,max} = q \cdot V'_{Ed,1}$ ), as was assumed by Keintzel. This yields an upper bound of the shear magnification factor  $\epsilon_{upper}$ , which is even higher than the seismic force reduction factor ( $\epsilon_{upper} > q$ ):

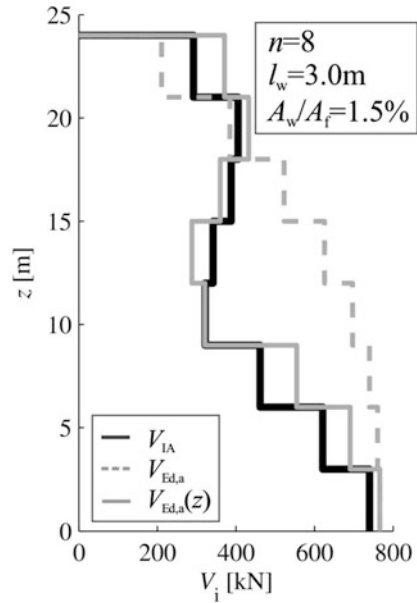
$$\epsilon_{upper} = \sqrt{q^2 + 0.1 \cdot \left( q \cdot \frac{S_e(T_C)}{S_e(T_1)} \right)^2} \tag{24.5}$$

and finally:

$$\epsilon_a = q \cdot \sqrt{\left( \min \left[ \frac{\gamma_{Rd}}{q} \cdot \frac{M_{Rd}}{M_{Ed}}; 1 \right] \right)^2 + 0.1 \cdot \left( \frac{S_e(T_C)}{S_e(T_1)} \right)^2} \geq 1.5 \tag{24.6}$$

Figure 24.5 graphically illustrates these two observations. If the expression for  $\epsilon$  proposed by Keintzel is applied to the total base shear (as it is understood from the ambiguous notation in Eurocode 8), the results are in general over-conservative (see the points marked by squares in Fig. 24.5). However, in the long period region the upper bound for the magnification factor applies, yielding a good match with the results of the inelastic analysis. On the other hand, the properly applied and

**Fig. 24.6** Distribution of shear forces over the height of the eight-storey wall as given by Eurocode 8 (the dashed line), the proposed formula (the solid grey line), and inelastic response analysis (the black line) (More data about the inelastic response analysis can be found in Rejec et al. 2012)



modified formula ( $\varepsilon_a$ ) yields a good correlation with the results of the inelastic analysis over the entire span of the periods involved (see the points marked by triangles in Fig. 24.5).

Eurocode 8 suggests that the same shear magnification factor should be used along the entire height of the wall. As expected, this could result in a substantial overestimation of the shear forces at mid-height, and an underestimation of the shear forces at the top, where the contribution of the higher modes is more pronounced than at the base. This observation is illustrated by means of a dashed line in Fig. 24.6 for one of the eight-storey walls analysed in the parametric study (the length of the wall  $l_w$  was 3 m, and the assumed wall-to-floor area ratio was 1.5 %).

To account for this variation along the height of the wall, it was proposed (Rejec et al. 2012) that the constant ratio between the contribution of the higher modes and the contribution of the first mode ( $\sqrt{0.1}$ ), which is approximately valid at the base of the wall, should be replaced by a variable ratio along the height –  $m(z)$  (Eq. 24.7).

$$\varepsilon_a(z) = q \cdot \sqrt{\left(\min \left[ \frac{\gamma_{Rd}}{q} \cdot \frac{M_{Rd}}{M_{Ed}}; 1 \right] \right)^2 + m(z)^2 \cdot \left( \frac{S_e(T_C)}{S_e(T_1)} \right)^2} \geq 1.5 \quad (24.7)$$

It was assumed that the distribution of this ratio  $m(z)$  was the same as in the case of the elastic flexural cantilever beam (fully realizing that this is only an approximation in the inelastic range, and that it is applicable only to regular walls with no plastic hinges in the upper storeys).

For the chosen eight-storey wall (for more complete results, see Rejec 2011) the results  $V_{Ed,a}(z)$  obtained by using  $\varepsilon_a(z)$  in combination with  $V_{Ed,1}'$  are presented in Fig. 24.6. The results are compared with the shear envelopes obtained by using inelastic response history analyses  $V_{IA}$  and the design shears obtained by multiplying  $V_{Ed,1}'$  with the constant  $\varepsilon_a(z=0)$  along the entire height (as suggested in Eurocode 8).

## 24.3 Numerical Modelling of the Inelastic Shear Response and Shear-Flexural Interaction in RC Structural Walls

### 24.3.1 Background

A reliable model for inelastic seismic shear response is still to be defined. For this reason many researchers ignore or try to avoid this problem. They frequently assume that shear failure in newly built walls is automatically prevented by capacity design. However, as has been shown in the previous section, the shear magnification factors have not yet been clearly defined, and many designers/codes even do not use them at all. In the case of the walls of older buildings, researchers try to avoid the problem by assuming elastic shear behaviour, and then making post-analyses checks. However, ignoring inelastic shear-flexural interaction makes the results of such analyses questionable. This is particularly true in the case of seismic risk analyses, where structures are analysed up to the near collapse stage. Improved models for inelastic shear response are therefore needed.

Some other models for inelastic shear-flexural interaction have already been proposed and experimentally verified, e.g. those proposed by Kabeyasawa (1997), Chen and Kabeyasawa (2000), Orakcal et al. (2006), and Kim et al. (2011). However, refinements in the description of the cyclic behaviour are still needed. Another concern is the complexity of some of the proposed models, which makes them difficult to apply to realistic structures.

In general, the research group at the University of Ljubljana has trust in macro models, even in the case of complex behaviour. Macro models are defined here as models which monitor force-displacement rather than stress-strain relationships. In the particular case of structural walls, the authors have used the multiple-vertical-line-element model – MVLEM (Fig. 24.7).

The model has been consistently proved to be efficient in the cases of a predominantly flexural response. For example, it was used in the case of the benchmark prediction for the “San Diego” wall that was awarded the “best prediction” recognition (EERI 2006). However, the research group has still not been able to completely understand and define the inelastic behaviour of shear springs and, first of all, the inelastic interaction of the shear and flexural springs in the model. This lack of knowledge was demonstrated during the “ECOLEADER” test of a coupled wall (Figs. 24.1 and 24.8) (Kante 2005; Fischinger et al. 2006). Due to



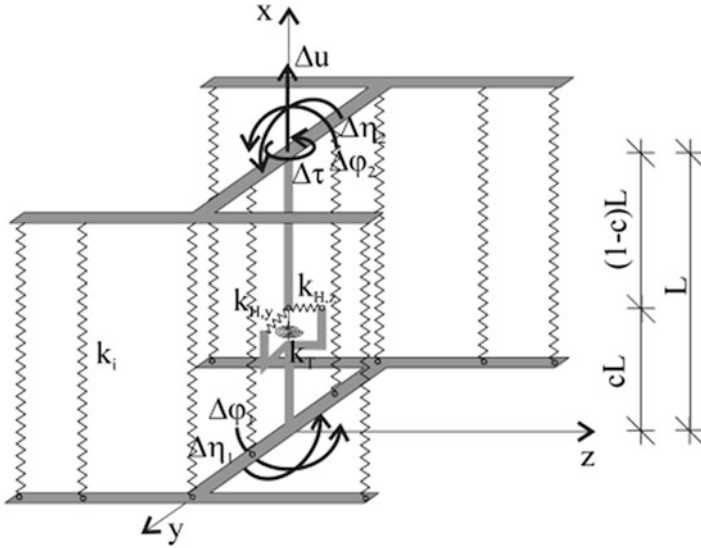


Fig. 24.7 3D multiple-vertical-line-element

Fig. 24.8 Shear failure of the piers in the ECOLEADER wall (see Fig. 24.1)



the overstrength of the coupling beams, large axial forces were induced in the piers, which subsequently failed due to shear-tension interaction. After the test, the use of the compression field theory (Vecchio and Collins 1986) substantially improved the analytical results (Kante 2005). However, the theory was found to be incomplete in the case of cyclic response.

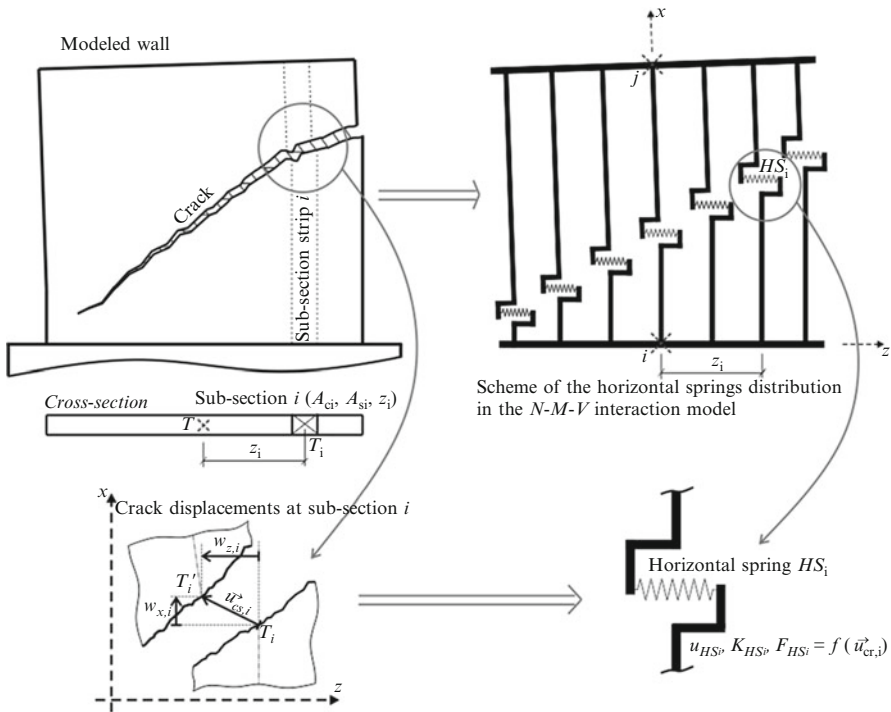


Fig. 24.9 Model accounting for inelastic shear and shear-flexural interaction in structural walls (the vertical springs are not shown)

### 24.3.2 Proposed Numerical Model

In order to account for the inelastic shear behaviour and the axial force – bending moment – shear force ( $N$ - $M$ - $V$ ) interaction better, the MVLEM was modified (Rejec 2011), and incorporated into the OpenSees program (McKenna and Fenves 2007). The modified element is illustrated in Fig. 24.9 (only the 2D element is shown in order to make the illustration clearer). In principle, one additional shear spring has been introduced into each of the vertical strips (springs), as proposed by Wallace (Orakcal et al. 2006).

The following key assumptions were considered in the development of the model:

- Cracks are straight and equally spaced. The (constant) spacing between cracks should be evaluated according to empirical procedures.
- The shear displacements of the element caused by the compressive deformation of the diagonal struts are neglected. It is assumed that the tensile and shear deformations in the cracked strips are localized in the cracks.

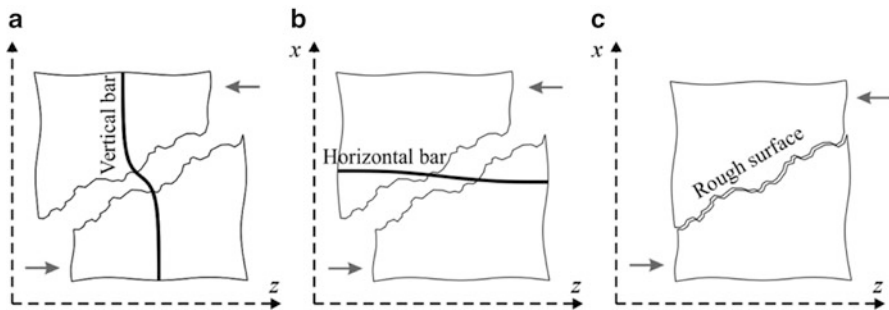


**Fig. 24.10** Mechanisms of shear force transfer across the cracks: (a) the dowel effect of the vertical reinforcement; (b) the axial resistance of the horizontal/shear reinforcement, and (c) aggregate interlock in the crack



**Fig. 24.11** Each horizontal spring consists of three components to account for aggregate interlock (HSA), the dowel effect (HSD), and the shear/horizontal reinforcement (HSS) mechanisms

- Along the height of the wall segment the inclination of the cracks and the displacement within different cracks is assumed to be constant.
- The current crack inclination is evaluated according to the average current strain state in the element, and is updated at every load step (the rotating-crack model).

The above assumptions have been empirically verified, and they are valid for walls with low to moderate compressive axial forces (typical for the European practice, see the Introduction). In other cases the compression strut is additionally checked.

The shear behaviour and resistance modelled by the horizontal springs depend on the mechanisms that transfer the shear force across the cracks (Fig. 24.10). The mechanisms consist of (a) the dowel effect of the vertical bars, (b) the axial resistance of the horizontal/shear bars, and (c) aggregate interlock, i.e. the interlocking of aggregate particles in the crack. The capacity of the latter is highly dependent on the width of the cracks.

Thus, each spring has three components (Fig. 24.11): HSA to account for aggregate interlocking, HSD to account for the dowel action, and HSS to account for the axial resistance of the shear reinforcement. The current characteristics of each component depend on the deformations/displacements at the crack within the individual strip. The displacements are linked to the current displacements of the nodes of the element.

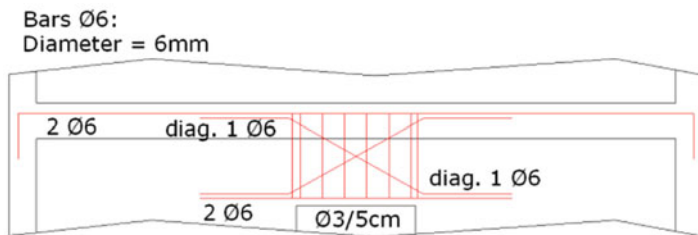


Fig. 24.12 Reinforcement in the coupling beams

The constitutive relations for the individual springs are based on the semi-empirical relations found in the literature (a detailed description is given in Rejec 2011). Aggregate interlock is modelled by the Lai-Vecchio model (Vecchio and Lai 2004), dowel action by the expressions proposed by Dulacska (1972), and by Vintzeleou and Tassios (1987). The force-displacement relation for the HSS springs is based on the bar-slip model proposed by Elwood and Moehle (2003).

### 24.3.3 Experimental Verification of the Proposed Model

The inelastic response of the wall presented in the introduction (Fig. 24.1) was analysed in order to verify the suitability of the proposed model. The 1:3 model of a five-storey wall (Fig. 24.1) consisted of two coupled T-shaped piers (Fischinger et al. 2006, 2008, 2010). The piers were reinforced by very light (minimum) reinforcement, according to the Slovenian building practice. The distributed mesh reinforcement amounted to 0.25 % of the cross-section in both directions. Note that the small diameter bars (3 mm) used for the reinforcement mesh in the model were very brittle (their ultimate strain was only 1.5 %). The coupling beams, too, were lightly reinforced (Fig. 24.12). A heavy additional mass was added due to the reduced scale, and to account for the mass in adjacent fields in realistic structures. This required a relatively thick slab, i.e. one with a thickness of 8 cm, which would be equal to 24 cm in the prototype structure.

The shaking table test was performed at LNEC in Lisbon, Portugal within the scope of the ECOLEADER project, which was coordinated by University of Ljubljana team. The Tolmezzo accelerogram, recorded during the 1976 Friuli earthquake, was used in two directions in a series of tests with increasing intensity. In the last of the series of the tests (the 6th run) the table acceleration in the direction of the web wall with openings was  $a_{g,max,X} = 1.02$  g, and the acceleration in the direction of the flange walls was  $a_{g,max,Y} = 0.52$  g. Failure occurred in the direction of the web (see Fig. 24.8 in Sect. 24.3.1). Typical shear failure of the wall piers was observed. The flange walls were only lightly damaged. Some damage was observed at the unconfined edges, and due to punching caused by the web wall. To the surprise of observers, the supposedly weak coupling beams were practically undamaged.

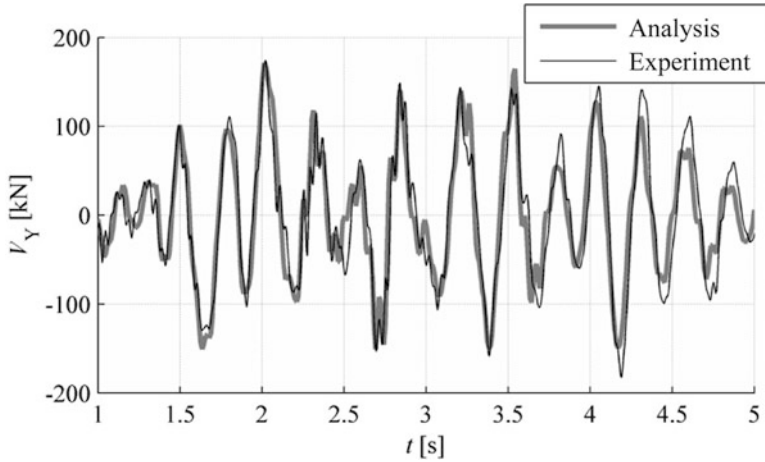


**Fig. 24.13** Base shear response in the direction of the web on the 5th run. Comparison of the numerically and experimentally obtained results

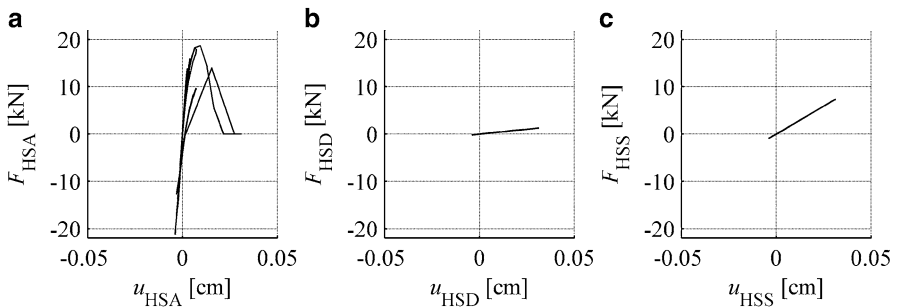


**Fig. 24.14** Response of the shear springs on the 5th run. (a) HSA indicates the deterioration of aggregate interlock in one direction. (b) the dowel spring HSD and (c) the shear reinforcement spring HSS were subsequently activated

No significant inelastic behaviour was detected in the first four runs, neither during the experiment, nor in the numerical model. A moderate inelastic response of the specimen was observed on the 5th run ( $a_{g,max,X} = 0.42 g$ ;  $a_{g,max,Y} = 0.73 g$ ), which was the one before the last. Considerable lifting of the piers due to strong coupling was observed. The vertical bars in the flanges yielded, the cracks in the flanges widened, and shear cracks formed in the webs of both piers in the first storey. The numerical model was able to reproduce the response very well. The nearly perfect match that was obtained in the case of the base shear response history (in the direction of the web) is shown in Fig. 24.13. The behaviour of one of the typical shear springs (the location of the spring is indicated in Fig. 24.1) is analysed in Fig. 24.14. When the web of the pier cracked, the aggregate interlocking mechanism

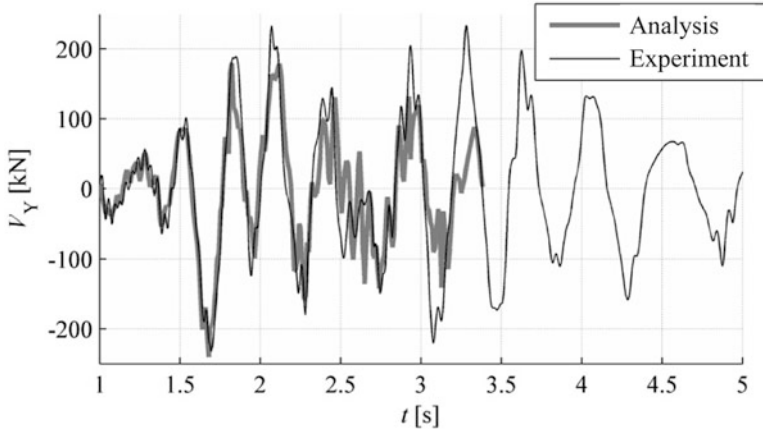


**Fig. 24.15** Base shear response in the direction of the web on the 6th run. Comparison of the numerically and experimentally obtained results

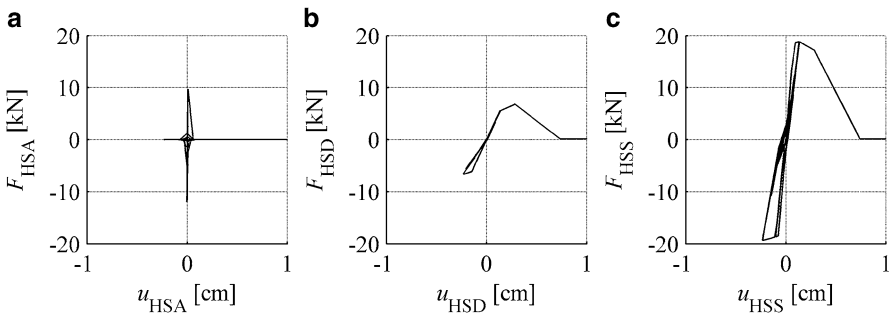
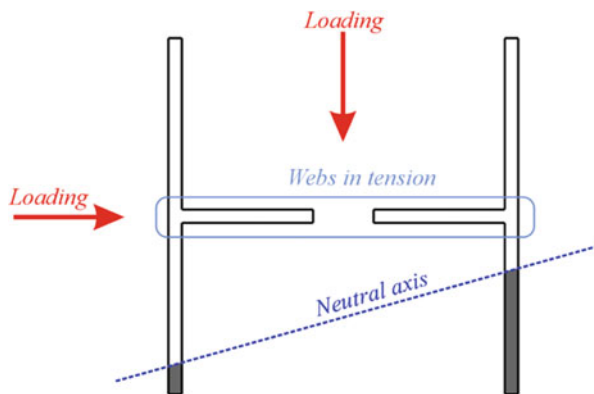


**Fig. 24.16** Response of the shear springs on the 6th run. (a) HSA indicates the complete loss of aggregate interlock. (b) The dowel mechanism HSD was fully activated and was then completely destroyed. (c) The shear reinforcement spring HSS yielded and then soon completely lost resistance (indicating rupture of the very brittle horizontal reinforcement)

was activated (Fig. 24.14a). After this interlocking mechanism had deteriorated, the horizontal reinforcement was activated (Fig. 24.14c). However, it remained elastic. The dowel mechanism, too, was activated, but its contribution was almost negligible (Fig. 24.14b), indicating that the gap within the crack had remained small.

In the last – 6th run both piers failed in shear, and large shear cracks opened up in the flanges of the first floor. This failure was successfully identified and modelled (Figs. 24.15 and 24.16). The aggregate interlocking mechanism, which had considerably deteriorated in the previous run, was completely destroyed (Fig. 24.16a), and the HSS spring indicated the rupture of the very brittle horizontal reinforcement (note the very short yield plateau in Fig. 24.16c), which was actually used in the test specimen. The dowel mechanism was first fully activated, and then failed completely (Fig. 24.16b).

**Fig. 24.17** The identified neutral axis position during the 6th run



The residual resistance of the wall observed in the test (and not numerically verified) can be attributed to the frame action of the flanges and slabs (which was not included in the model). The simultaneous and similar failure of the webs in both piers was attributed to the bi-axial loading. The results of the analysis showed that, at the time of the failure, the webs in both piers were in net tension (Fig. 24.17), which explains the same inclination of the crack in both piers.

## 24.4 Conclusions

During the inelastic response, shear forces in RC structural walls can be much larger than those predicted by equivalent elastic design procedures. The magnification, which is due to overstrength and the effect of higher modes, can be frequently close in size to the seismic force reduction factor.

The shear modification factor  $\varepsilon$  proposed in Eurocode 8 for ductile walls (ductility class high) was found to be adequate at the base of walls, providing that it was properly applied (to the base shear contributed by the first mode only) and the upper bound of the modification factor required by the code was increased.

Eurocode 8 assumes constant amplification along the height of the wall, which is conservative at the mid-height and rather unconservative at the top. A variable amplification factor along the height was proposed.

Although the phenomenon of the increasing inelastic shear has been known for a long time, many walls with insufficient shear resistance have been designed in the past and even today. A model is therefore needed to account for inelastic shear behaviour and inelastic shear-flexural interaction.

Such model has been proposed. It is based on the multiple-vertical-line-element macro model. An additional shear spring, which accounts for aggregate interlock, the dowel action, and horizontal reinforcement resistance, is incorporated into each of the vertical springs.

The current characteristics of each component depend on the deformations at the crack (in particular the width of the crack) within the individual strip. The constitutive relations for the individual springs are based on the semi-empirical relations found in the literature. Aggregate interlock is modelled by the Lai-Vecchio model (Vecchio and Lai 2004), whereas the dowel action is modelled by expressions proposed by Dulacska (1972), and Vintzeleou and Tassios (1987). The force-displacement relation for HSS springs is based on the bar-slip model proposed by Elwood and Moehle (2003).

The model successfully simulated the response of a five-storey coupled wall tested on the shaking table under bi-axial excitation. The shear resisting mechanisms within the cracks were adequately modelled up to the tension shear failure of both piers.

## References

- Blakeley RWG, Cooney RC, Megget LM (1975) Seismic shear loading at flexural capacity in cantilever wall structures. *Bull N Z Natl Soc Earthq Eng* 8(4):278–290
- Boroschek R, Bonelli P (2014) Lessons from the Chile 2010 earthquake for performance based design and code development. In: Fischinger M, Stojadinović B (ed) *Performance-based seismic engineering – vision for an earthquake resilient society*. Springer
- CEN (2004) Eurocode 8 – design of structures for earthquake resistance. Part 1: general rules, seismic actions and rules for buildings. European standard EN 1998–1, Dec 2004, European Committee for Standardization, Brussels
- Chen S, Kabeyasawa T (2000) Modeling of reinforced concrete shear wall for nonlinear analyses. In: *Proceedings of the 12th WCEE, New Zealand Society of Earthquake Engineering, Auckland*
- Dulacska H (1972) Dowel action of reinforcement crossing cracks in concrete. *ACI Struct J* 69(12):754–757
- EERI (2006) News of the membership – blind prediction contest winners. *EERI Newslett* 40(9):4
- Elwood KJ, Moehle JP (2003) Shake table tests and analytical studies on the gravity load collapse of reinforced concrete frames, PEER report 2003/01, University of California, Berkeley, EERI Newslett (2006), 40(9):4
- Fischinger M, Isaković T, Kante P (2006) Shaking table response of a thin H-shaped coupled wall. In: *Managing risk in earthquake country – 100th anniversary earthquake conference: centennial meeting, San Francisco*. Earthquake Engineering Research Institute, Berkeley, CD ROM
- Fischinger M, Kramar M, Isaković T, (2008) Using macro elements to predict near-collapse performance of two typical RC building structural systems with lightly reinforced walls and slender precast columns. In: *Proceedings of the 14th world conference on earthquake engineering, Beijing, CD ROM*
- Fischinger M, Rejec K, Isaković T (2010) Seismic behavior of RC structural walls and Eurocode 8 provisions. In: *Proceedings of the 9th US National and 10th Canadian conference on earthquake engineering, Oakland, Earthquake Engineering Research Institute, Canadian Association for Earthquake Engineering, Ottawa*
- Kabeyasawa T (1997) Design of RC shear walls in hybrid wall system. In: *Proceedings, Fourth Joint Technical Coordinating Committee, U.S.-Japan cooperative seismic research on composite and hybrid structures, Monterey*
- Kante P (2005) Seismic vulnerability of RC structural walls (in Slovenian). Ph.D. Dissertation, University of Ljubljana



- Keintzel E (1990) Seismic design shear forces in RC cantilever shear wall structures. *Eur Earthq Eng* 3:7–16
- Kim Y, Kabeyasawa T, Matsumori T, Kabeyasawa T (2011) Numerical study of a full-scale six-storey reinforced concrete wall-frame structure tested at E-Defense. *Earthq Eng Struct Dyn* 41(8):1217–1239. doi:10.1002/eqe.1179
- McKenna F, Fenves GL (2007) Open system for earthquake engineering simulation, Pacific Earthquake Engineering Research Center, Berkeley <http://opensees.berkeley.edu>
- Orakcal K, Massone LM, Wallace JW (2006) Analytical modeling of reinforced concrete walls for predicting flexural and coupled shear-flexural responses, PEER report 2006/07. University of California, Berkeley
- Rejec K (2011) Inelastic shear behaviour of RC structural walls under seismic conditions (in Slovenian). PhD dissertation, University of Ljubljana
- Rejec K, Isaković T, Fischinger M (2012) Seismic shear force magnification in RC cantilever structural walls, designed according to Eurocode 8. *Bull Earthq Eng* 10(2):567–586. doi:10.1007/s10518-011-9294-y
- Vecchio FJ, Collins MP (1986) The modified compressional-field theory for reinforced concrete elements subjected to shear. *ACI J* 83(2):219–231
- Vecchio FJ, Lai D (2004) Crack shear-slip in reinforced concrete elements. *J Adv Concr Technol* 2(3):289–300
- Vintzeleou EN, Tassios TP (1987) Behavior of dowels under cyclic deformations. *ACI J* 84(1): 18–30
- Wallace JW, Moehle JP (1993) Evaluation of ductility and detailing requirements of bearing wall buildings using data from the March 3, 1985, Chile earthquake. *Earthq Spectra* 9(1):137–156
- Wood SL (1991) Performance of reinforced concrete buildings during the 1985 Chile earthquake: implications for the design of structural walls. *Earthq Spectra* 7(4):607–638